864. Energy analysis of multiple-cracked Euler-Bernoulli beam

Amin Ghadami[1], Ameneh Maghsoodi[2], Hamid Reza Mirdamadi[3]
[1]Department of Mechanical Engineering, Sharif University of Technology, Tehran 11155-8639, Iran
[2]Department of Mechanical Engineering, Amirkabir University of Technology, Tehran 15875-4413, Iran
[3]Department of Mechanical Engineering, Isfahan University of Technology, Isfahan 84156-83111, Iran
Corresponding author: Tel: +989133163147; Fax: +983113912628
E-mail: [1]*ghadami_amin@mech.sharif.ir*, [2]*a_maghsoodi@aut.ac.ir*, [3]*hrmirdamadi@cc.iut.ac.ir*
(Received 7 July 2012; accepted 4 September 2012)

Abstract. This paper presents energy analysis of multiple-cracked beams. The study deals with crack energy reduction functions for consuming strain energy due to crack growth and the degree of conformity between these functions and experimental results. Three different reduction functions are employed in this research work. A comprehensive analysis is performed providing a comparison of the functions for a beam with one and two cracks. In order to elucidate advantages and disadvantages of each function, we employ them in different crack detection problems. For different cases of crack localization and quantification in a crack detection problem, the best function that fits the experimental results more accurately is highlighted.

Keywords: crack detection, multiple-cracked beam, crack energy reduction function, modified rotational flexibility, crack interaction.

Nomenclature

a_i	i^{th} crack depth
b	Beam width
D	Local rotational flexibility
$D^{'}$	Local modified rotational flexibility
E	Beam Young's modulus
$f(\gamma_i)$	Correction function for i^{th} crack with normalized depth γ_i
h	Beam height
I	2^{nd} static moment of the beam cross-sectional area
$k(\gamma_i)$	Local angular stiffness of a massless rotational spring at the inserted crack location
L	Beam length
$M_n(\beta_i)$	Resisting modal bending moment developed in the mode n and crack location β_i
$R^{(n)}$	Energy reduction function
T_n	Total modal kinetic energy of the uncracked beam in the n^{th} mode per ω_n^2
$\overline{T}_{n,m}$	Total modal kinetic energy of the cracked beam in the n^{th} mode per $\overline{\omega}_n^2$ due to m cracks
$\overline{U}_n$	Total modal strain energy stored in the cracked beam in the mode n
ΔU_n	Local modal energy reduction in beam strain energy at mode n due to a multiple-crack model
$\Delta U_{n,m}^i$	Local modal energy reduction in beam modal strain energy at mode n due to m cracks for the i^{th} crack

$\Delta U^{'}$	Modified energy consumed for the crack growth
x	Cartesian coordinate along beam length
$\phi_n(\beta)$	Transverse mode shape of the uncracked beam in the n^{th} mode
$\phi_n^{"}(\beta)$	Curvature of the n^{th} mode shape of the uncracked beam
ω_n	The n^{th} mode undamped natural frequency of uncracked beam
$\overline{\omega}_n$	The n^{th} mode undamped natural frequency of cracked beam
ρ	Mass density of beam (per unit volume)
$\beta_i = x_i/L$	Normalized i^{th} crack location
$\gamma_i = a_i/h$	Normalized i^{th} crack depth
$\Gamma_{c,p}^n$	Energy reduction caused by crack "c" in part "p" in the n^{th} mode

1. Introduction

One of the main causes of structural failure is the existence of cracks in structures. Non-destructive testing (NDT) methods such as ultrasonic testing, *X*-ray, acoustic emission (AE), acousto-ultrasonic, Lamb waves, etc. [1] generally use NDT techniques for localized inspection and monitoring of damages in structures. Because of some inconveniences in using these methods, such as structures with limited accessible parts, vibration-based methods have attracted attention of researchers [2]. In the vibration-based methods, many researchers investigated the effect of cracks on vibrational characteristics, such as Jialou Hu et al. [3], Sekhar [4], and others [5-10]. Among the structures, the most investigated structure in the vibration-based methods is a beam-like structure. In the majority of studies, a beam is modeled based on Euler-Bernoulli theory [1-10].

However, Timoshenko beam theory is used in some research works [11-13]. On the other side, most of researchers analyzed a beam with only a single crack [11-20]. However, several researchers have also considered multiple-cracked beams [21-27]. In most of these studies, it was assumed that the effect of a crack was concentrated at the crack location. However, some researchers suggested a distribution function along the beam for energy reduction caused by a crack. Yang et al. [28] suggested a distribution function using an energy method. Behzad et al. [29] developed a distribution function as a crack disturbance function for a crack using fracture mechanics. Mazanoglu et al., [30, 31], used the distribution function presented in the reference [28] for vibration analysis of a multiple-cracked non-uniform beam. In these studies, Mazanoglu et al. [30, 31] suggested some modifications in the prevalent crack energy reduction function for a single and multiple-cracked beam.

In this study, we make a comparison between the prevalent (unmodified) energy reduction function and the other two modified versions suggested according to theories presented in [30, 31]. We study Euler-Bernoulli beams with one and two cracks, and investigate the effect of the suggested modifications in the formulations. Further, we clarify whether these modifications lead to more accurate results in crack detection problems.

2. Formulation

In this section, we formulate relationships between modal parameters and geometric parameters of cracks. We consider the lateral vibrations of prismatic beam-like structures modeled by Euler-Bernoulli kinematics and linear elastic constitutive Hooke's law.

2.1. Single-cracked formulation

As shown in Fig. 1, we assume there is an open single-side crack with a total depth a_1, in a normal cross-section at $x = x_1$. Due to a crack, the beam elastic strain energy reduces locally. According to the linear elastic fracture mechanics (LEFM) theory, we can represent this reduction as follows [10]:

$$\Delta U = \frac{M^2(\beta_1)}{2k}\ , \tag{1}$$

where M is bending moment at the crack cross section $\beta_1 = x_1/L$, and k is a local rotational stiffness of the beam at the crack location and is defined as follows [10]:

$$k(\gamma_1) = \frac{Ebh^2}{72\pi f(\gamma_1)}\ , \tag{2}$$

where $\gamma = \frac{a_1}{h}$. The correction function, $f(\gamma)$, is represented in the following form:

$$f(\gamma) = 0.6384\gamma^2 - 1.035\gamma^3 + 3.7201\gamma^4 - 5.1774\gamma^5 + 7.553\gamma^6 - 7.3324\gamma^7 + 2.4909\gamma^8 \tag{3}$$

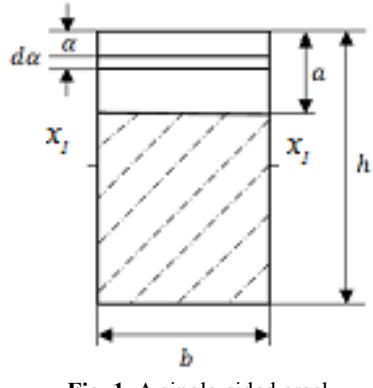

Fig. 1. A single-sided crack

This relation is accurate enough for $\gamma \le 0.6$ [27]. We can represent Eq. (1) in the following form [30]:

$$\Delta U(\beta_1, \gamma_1) = D(\gamma_1) M^2(\beta_1)\,, \tag{4}$$

where:

$$D(\gamma_1) = \frac{36\pi f(\gamma_1)}{Ebh^2}\,. \tag{5}$$

We call D as a local rotational flexibility at the crack location β_1. We can also calculate the n^{th} undamped natural frequency of uncracked beam using Rayleigh's quotient as follows:

$$\omega_n^2 = \frac{U_n}{T_n}, \tag{6}$$

where:

$$U_n = \frac{L}{2}\int_0^1 EI\left[\phi_n''(\beta)\right]^2 \mathrm{d}\beta, \tag{7}$$

$$T_n = \frac{L}{2}\int_0^1 \rho A\, \phi_n^2(\beta)\mathrm{d}\beta. \tag{8}$$

Similar to uncracked beam, for the cracked beam we have:

$$\overline{\omega}_n^2 = \frac{\overline{U}_n}{\overline{T}_n} = \frac{\overline{U}_{n,1}}{\overline{T}_{n,1}}, \tag{9}$$

where:

$$\overline{U}_n(\beta_1,\gamma_1) = U_n - \Delta U_{n,1}. \tag{10}$$

For a beam with a normal edge crack of small depth, there is no noticeable change in the mass before and after cracking. Therefore we may assume that the transverse mode shapes of the uncracked and cracked beams are the same [3, 27]. Accordingly, based on Eq. (8), we may hypothesize:

$$T_n = \overline{T}_n = \overline{T}_{n,1}. \tag{11}$$

Substituting Eq. (10) and (11) into Eq. (9) we find:

$$\overline{\omega}_{n,1}^2 = \frac{U_n - D(\gamma_1)M_n^2(\beta_1)}{T_n}. \tag{12}$$

By combining Eq. (6) and (12), we obtain:

$$\frac{\omega_n^2 - \overline{\omega}_{n,1}^2}{\omega_n^2} = \frac{D(\gamma_1)M_n^2(\beta_1)}{U_n}. \tag{13}$$

If we assume that $\omega_n + \overline{\omega}_{n,1} \cong 2\omega_{n,1}$ and $\omega_n - \overline{\omega}_{n,1} \cong \Delta\omega_{n,1}$, we can approximate Eq. (13) as follows:

$$\frac{\Delta\omega_{n,1}}{\omega_n} \cong \frac{D(\gamma_1)M_n^2(\beta_1)}{2U_n}. \tag{14}$$

In addition, from the generalized Hooke's law of simple beam theory:

$$M_n(\beta_1) = EI\,\phi_n''(\beta_1). \tag{15}$$

2.1. Multiple-cracked formulation

Using the equations presented in the previous section, we can generalize Eq. (4) for m cracks based on an energy reduction in each modal strain energy [27]:

$$\Delta U_{n,m} = \sum_{i=1}^{m} \Delta U_{n,i} = \sum_{i=1}^{m} D(\gamma_i) M_n{}^2(\beta_i). \tag{16}$$

In addition, we can generalize Eq. (13) and (14) in the following forms:

$$\frac{\omega_n^2 - \overline{\omega}_{n,m}^2}{\omega_n^2} = \frac{\sum_{i=1}^{m} D(\gamma_i) M_n{}^2(\beta_i)}{U_n}, \tag{17}$$

$$\frac{\Delta\omega_{n,m}}{\omega_n} = \frac{\sum_{i=1}^{m} D(\gamma_i) M_n{}^2(\beta_i)}{2U_n}. \tag{18}$$

2.3. Modifications

In this section, we describe two modifications for the above formulations. We can apply and investigate each of these modifications separately or together.

2.3.1. The first modification

As a first modification, we can consider a modified value for $D(\gamma_i)$ as follows [30]:

$$D'(\gamma_i) = D(\gamma_i)(1-\gamma_i). \tag{19}$$

We call $D'(\gamma_i)$ a modified rotational flexibility. Therefore, a modified energy consumed due to the crack growth can be represented as follows:

$$\Delta U'_{n,i} = D'(\gamma_i) M_n^2\ (\beta_i) = D(\gamma_i)(1-\gamma_i) M_n^2(\beta_i). \tag{20}$$

Therefore, according to this suggested modification we can rewrite Eq. (18) in the following form:

$$\frac{\Delta\omega_{n,m}}{\omega_n}=\frac{\sum_{i=1}^{m}D'(\gamma_i)M_n^2(\beta_i)}{2U_n}=\frac{\sum_{i=1}^{m}D(\gamma_i)(1-\gamma_i)M_n^2(\beta_i)}{2U_n}. \tag{21}$$

2.3.2. The second modification

Another modification is suggested for multiple-cracked beam cases [30]. In this suggestion, the effect of each crack is not only a reduction in the strain energy, but also an increase in strain energy due to multi-crack interaction. For example, for a triple-cracked beam, the energy distribution diagram is presented in Fig. 2 [30]. In this diagram, the energy consumed (*CE*) due to single-crack growth, distributed along the beam, using the distribution function suggested by Yang et al. [28], is as follows (the notation has been changed for conformity with this research):

$$\Gamma^{n,i}=\frac{\varphi_n(\gamma_i,\beta_i)}{1+\left[L(\beta-\beta_i)/(q(\gamma_i)h\gamma_1)\right]^2}, \tag{22}$$

$$\varphi_{n,i}(\gamma_i,\beta_i)=\frac{D(\gamma_i)\left[M(\beta_i)\right]^2}{q(\gamma_i)h\gamma_i\left[\arctan\left[L(1-\beta_i)/(q(\gamma_i)h\gamma_i)\right]+\arctan\left[L\beta_i/(q(\gamma_i)h\gamma_i)\right]\right]}, \tag{23}$$

$$q(\gamma_i)=\frac{6f(\gamma_i)(1-\gamma_i)^3}{\gamma_i(1-(1-\gamma_i)^3)}. \tag{24}$$

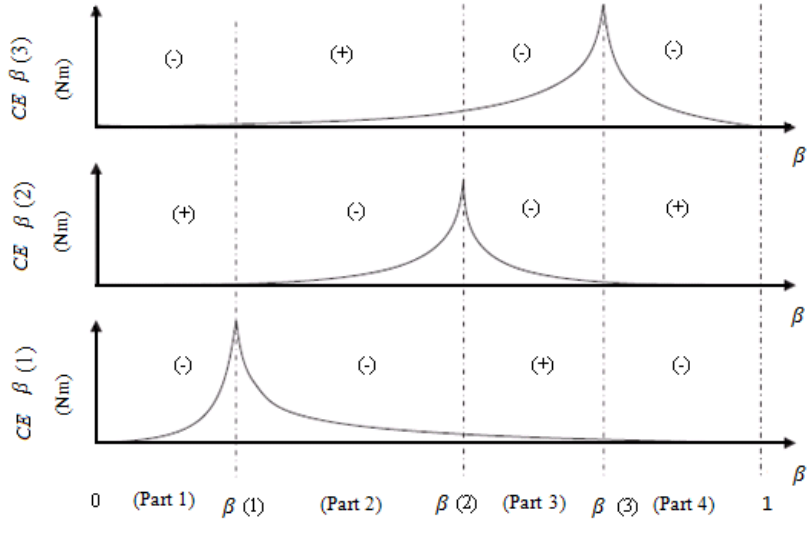

Fig. 2. Distribution diagram of crack energy consumed and crack interaction for a triple-cracked beam. (The Figure is extracted from [30] with some notational changes)

In Fig. 2, the cracks cause a decrease in the strain energy in areas marked by "-" and an increase in the strain energy in areas marked by "+".

For example, for a double-cracked beam, we can modify the strain energy of the beam, according to Fig. 3:

$$\overline{U}_{n,2} = U_n - \Gamma_{1,1}^{(n)} - \Gamma_{1,2}^{(n)} - \Gamma_{2,2}^{(n)} - \Gamma_{2,3}^{(n)} + \Gamma_{1,3}^{(n)} + \Gamma_{2,1}^{(n)}, \tag{25}$$

$$\Delta U_{n,2} = \Gamma_{1,1}^{(n)} + \Gamma_{1,2}^{(n)} + \Gamma_{2,2}^{(n)} + \Gamma_{2,3}^{(n)} - \Gamma_{1,3}^{(n)} - \Gamma_{2,1}^{(n)}, \tag{26}$$

where $\Gamma_{c,p}^{(n)}$ is the energy reduction caused by crack "*c*" in part "*p*" in the n^{th} mode shape of the beam. For example, for $\Gamma_{2,3}^{(n)}$ we have:

$$\Gamma_{2,3}^{(n)} = L\int_{\beta_2}^{\beta_3} \frac{\varphi(\gamma_2,\beta_2)}{1+\left[L(\beta-\beta_2)/(q(\gamma_2)h\gamma_2)\right]^2} d\beta \tag{27}$$

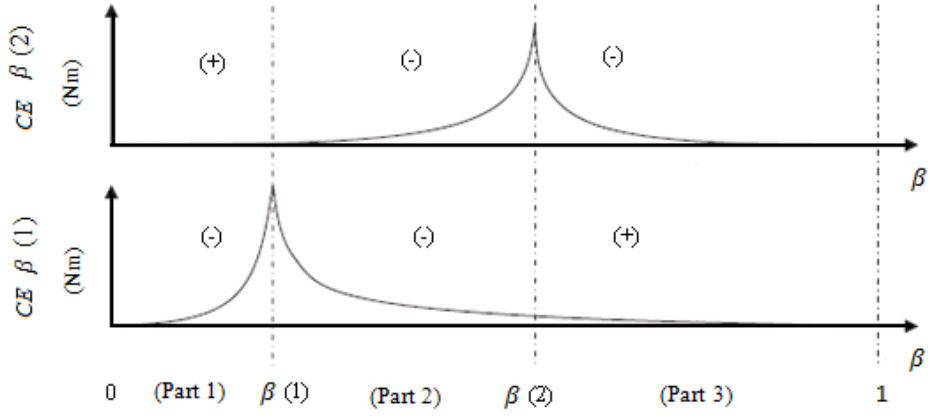

Fig. 3. Distribution diagram of crack energy consumed and crack interaction for a double-cracked beam

In the following sections, we make a comparison between unmodified and modified equations and investigate the effects of each modification on the results.

3. Solution procedures

In the multi-crack detection problems, we use the following equation:

$$\frac{\Delta\omega_{n,m}}{\omega_n} = \frac{\Delta U_{n,m}(\gamma_i,\beta_i)}{2U_n}. \tag{28}$$

In this equation, we can obtain $\frac{\Delta\omega_{n,m}}{\omega_n}$ by measuring natural frequencies of intact and cracked beam. We can also compute U_n using intact beam mode shapes. Thus, if we rewrite Eq. (28) as:

$$2\frac{\Delta\omega_{n,m}}{\omega_n}U_n = \Delta U_{n,m}(\gamma_i,\beta_i), \tag{29}$$

where the left-hand side is known. The other side of this equation, $\Delta U_{n,m}(\gamma_i,\beta_i)$, is the modal strain energy reduction of the beam due to cracks. The more accurate the estimate of energy reduction function is, the closer the values of $\Delta U_{n,m}(\gamma_i,\beta_i)$ will be to the left-hand side of Eq. (29) by substituting the location and depth of the cracks involved. For our solution procedure, we define two other functions and parameters as follows:

$$W^{(n,m)} = 2U_n\frac{\Delta\omega_{n,m}}{\omega_n}, \tag{30}$$

$$R_j^{(n,m)} = \Delta U_{n,m}(\gamma_i,\beta_i),\ j=1,\ 2,\ 3. \tag{31}$$

where the subscript j denotes the type of prevalent energy reduction function or its modified versions. As we discussed earlier, the closer the values of functions $R_j^{(n,m)}$ and experimental values, $W^{(n,m)}$, the more accurate the crack detection results will be.

In the following sections, we make a comparison between the common unmodified and modified functions for a beam containing one and two cracks. We investigate the closeness of each of the functions $R_j^{(n,m)}$ with experimental values $W^{(n,m)}$ in all cases.

3.1. Single-cracked beam

For a single-cracked beam, consider prevalent (unmodified) energy reduction function as follows:

$$R_1^{(n,1)} = D(\gamma_1)M_n^2(\beta_1), \tag{32}$$

or, we can write Eq. (29) as follows:

$$W^{(n,1)} = 2U_n\frac{\Delta\omega_{n,1}}{\omega_n} = D(\gamma_1)M_n^2(\beta_1). \tag{33}$$

Applying the first modification (Section 2.3.1) in $R_1^{(n,1)}$ we get:

$$R_2^{(n,1)} = D(\gamma_1)(1-\gamma_1)M_n^2(\beta_1). \tag{34}$$

Note that in single-crack situations, we have no mutual interaction among the cracks, so the second modification is inapplicable.

3.2. Double-cracked beam

We can express the unmodified energy function for double-cracked beam as follows:

$$R_1^{(n,2)} = D(\gamma_1)M_n^2(\beta_1) + D(\gamma_2)M_n^2(\beta_2) \tag{35}$$

Applying the first modification to the above equation we obtain:

$$R_2^{(n,2)} = D(\gamma_1)(1-\gamma_1)M_n^2(\beta_1) + D(\gamma_2)(1-\gamma_2)M_n^2(\beta_2). \tag{36}$$

For the second modification, according to Fig. 3 that is presented for a double-cracked beam, we can obtain:

$$R_3^{(n,2)} = \Gamma_{1,1}^n + \Gamma_{1,2}^n + \Gamma_{2,2}^n + \Gamma_{2,3}^n - \Gamma_{1,3}^n - \Gamma_{2,1}^n \tag{37}$$

Note that to obtain Γ^n values, we use the modified flexibility $D^{'}(\gamma_i)$ as in the ref. [30]. In other words, in $R_3^{(n,m)}$ function both of suggested modifications are employed.

4. Numerical examples

4.1. Single-cracked beam

In this section, we use a beam with material and geometric specifications presented in [21]: $E = 210$ Gpa, $\rho = 7860$ kg/m^3, $h = 0.02$ m, $b = 0.012$ m, $L = 0.24$ m.

We leave a crack with different depths $\gamma = 0.1,\ 0.3,\ 0.5$ at different locations $\beta = 0.1,\ 0.2,\ ...,\ 0.8$ in the beam. We obtain natural frequencies for each case using FE software and compute the energy values of $W^{(n,1)}$, $R_1^{(n,1)}$ and $R_2^{(n,1)}$ for each case. The results are presented in Figs. 4(a-c) and Figs. 5(a-c). In these figures, the energy values are shown on the vertical axis by "ψ". The horizontal axis shows the normalized crack locations.

4.2. Double-cracked beam

In this example, we utilize the same beam as in the previous example. To solve this example, we use even cases of Table presented in [21] for double-cracked beam (Table 1). We compute energy values of $W^{(n,2)}$, $R_1^{(n,2)}$, $R_2^{(n,2)}$ and $R_3^{(n,2)}$ for each case and for the first four modes. The results are presented in Table 2.

Table 1. Natural frequencies obtained by FE analysis in [21] for double-cracked cantilever beam

Case no.	Crack locations and sizes				Natural frequencies (Hz)			
	Crack no. 1		Crack no. 2					
	β_1	γ_1	β_2	γ_2	ω_1	ω_2	ω_3	ω_4
	Uncracked beam		Analytical		289.925	1816.931	5087.459	9969.389
			FEM		288.670	1751.346	4680.559	8641.520
2	0.1	0.35	0.4	0.15	248.039	1654.086	4611.596	8581.089
4	0.15	0.40	0.45	0.5	229.482	1405.505	4445.952	7336.405
6	0.2	0.5	0.5	0.4	222.321	1527.623	4197.771	7122.095
8	0.25	0.2	0.55	0.45	271.594	1476.876	4435.421	7866.328

$E = 210$ Gpa, $\rho = 7860$ kg/m^3, $h = 0.02$ m, $b = 0.012$ m, $L = 0.24$ m

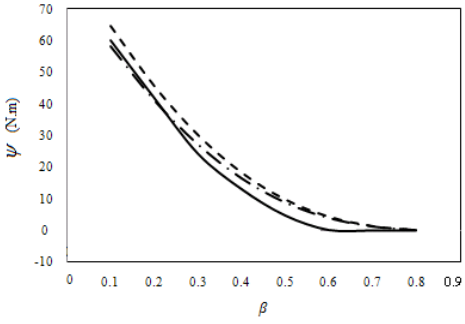

Fig. 4.a. $\gamma = 0.1$

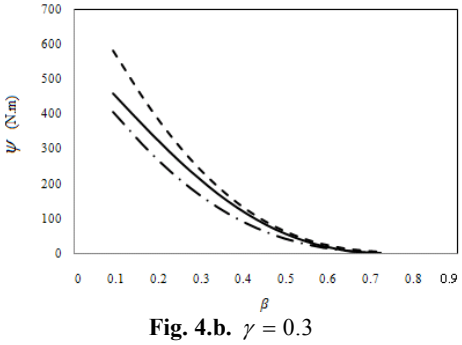

Fig. 4.b. $\gamma = 0.3$

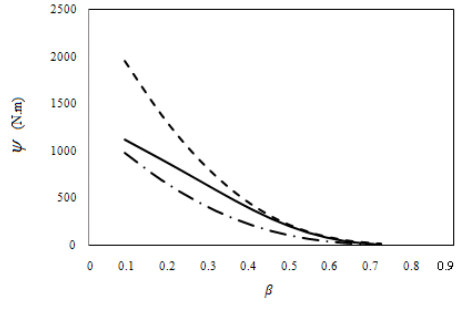

Fig. 4.c. $\gamma = 0.5$

Fig. 4. Diagram of ψ versus β in the first mode

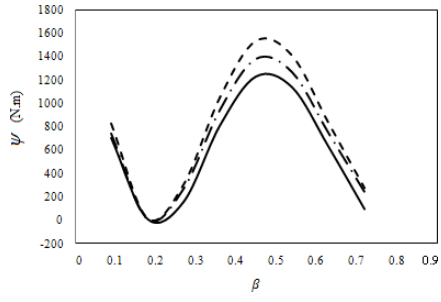

Fig. 5.a. $\gamma = 0.1$

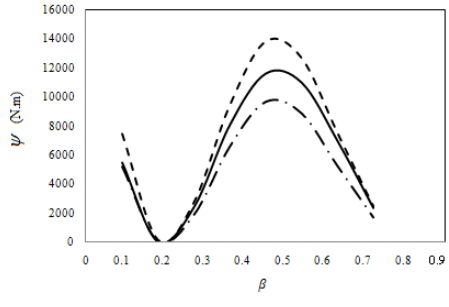

Fig. 5.b. $\gamma = 0.3$

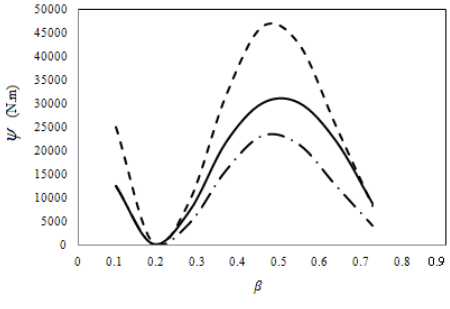

Fig. 5.c. $\gamma = 0.5$

Fig. 5. Diagram of ψ versus β in the second mode

(Solid, dashed and dash-dotted lines denote W, R_1 and R_2, respectively.)

Table 2. Relative difference percentages of $R_j^{(n,2)}$ functions from $W^{(n,2)}$

Case no.	First mode			Second mode			Third mode			Fourth mode		
	$e_1{}^a$	e_2	e_3	e_1	e_2	e_3	e_1	e_2	e_3	e_1	e_2	e_3
2	34	11.5	13.3	30.3	10.6	12.1	19.5	12.1	13.7	48.5	57.5	57.9
4	51	13.8	15.2	40.6	28.3	29.2	34.8	66.7	67	38.8	27.4	28.2
6	55	20.5	21.7	24.6	25.5	25.5	27.2	63.6	64.2	77.4	4.2	5.6
8	8.6	27.4	28.4	37.4	24.2	25.4	2.9	36.9	37.8	54	9.6	10.6

$^a e_i = \left| \frac{W - R_j}{W} \times 100 \right|$

4.3. Crack detection problem

In this section, in order to elucidate above results and use these results in an experimental problem, we provide several crack detection problems. We present these examples for single and double cracked beams using $R_1^{(n,m)}$, $R_2^{(n,m)}$ and $R_3^{(n,m)}$ functions in each case. We use a MATLAB program to solve these problems and provide the results in Tables 3 and 4.

Table 3. Comparison of predicted and simulated crack locations and sizes for single-cracked cantilever beam of section 4.1

Case no.	Simulated data		Predicted data using R_1		Predicted data using R_2	
	β	γ	β	γ	β	γ
1	0.2	0.1	0.202 {0.2%}[a]	0.096 {-0.4%}	0.202 {0.2%}	0.102 {0.2%}
2	0.4	0.1	0.406 {0.6%}	0.085 {-1.5%}	0.406 {0.6%}	0.090 {-1%}
3	0.3	0.2	0.298 {-0.2%}	0.187 {-1.3%}	0.298 {-0.2%}	0.212 {1.2%}
4	0.5	0.2	0.510 {1%}	0.187 {-1.3%}	0.510 {1%}	0.211 {1.1%}
5	0.4	0.3	0.396 {-0.4%}	0.283 {-1.7%}	0.396 {-0.4%}	0.342 {4.2%}
6	0.6	0.3	0.600 {0%}	0.281 {-1.9%}	0.600 {0%}	0.339 {3.9%}
7	0.5	0.4	0.476 {-2.4%}	0.360 {-4%}	0.476 {-2.4%}	0.468 {6.8%}
8	0.8	0.4	0.819 {1.9%}	0.458 {5.8%}	0.789 {-1.1%}	0.495 {9.5%}
9	0.4	0.5	0.383 {-1.7%}	0.454 {-4.6%}	0.395 {-0.5%}	0.710 {21%}
10	0.1	0.5	0.108 {0.8%}	0.405 {-9.5%}	0.108 {0.8%}	0.562 {6.2%}

$E = 210$ Gpa, $\rho = 7860$ kg/m^3, $h = 0.02$ m, $b = 0.012$ m, $L = 0.24$ m

[a]Relative percentage errors of prediction

Table 4. Comparison of predicted and simulated crack locations and sizes for double-cracked beam cases of Table 1

Case no.	Predicted data using R_1				Predicted data using R_2				Predicted data using R_3			
	β_1	γ_1	β_2	γ_2	β_1	γ_1	β_2	γ_2	β_1	γ_1	β_2	γ_2
3	0.110 {1%}[a]	0.225 {-2.5%}	0.466 {-3.4%}	0.257 {0.7%}	0.110 {1%}	0.260 {1%}	0.466 {-3.4%}	0.304 {5.4%}	0.110 {1%}	0.270 {2%}	0.466 {-3.4%}	0.307 {5.7%}
5	0.207 {0.7%}	0.258 {-4.2%}	0.462 {-3.8%}	0.373 {-2.7%}	0.207 {0.7%}	0.305 {0.5%}	0.462 {-3.8%}	0.493 {9.3%}	0.207 {0.7%}	0.320 {2%}	0.462 {-3.8%}	0.507 {10.7%}
7	0.271 {2.1%}	0.253 {0.3%}	0.545 {-0.5%}	0.278 {-2.2%}	0.271 {2.1%}	0.300 {5%}	0.545 {-0.5%}	0.334 {3.4%}	0.271 {2.1%}	0.310 {6%}	0.545 {-0.5%}	0.345 {4.5%}
9	0.338 {-1.19%}	0.342 {-0.8%}	0.601 {0.1%}	0.401 {-9%}	0.338 {-1.19%}	0.436 {8.6%}	0.601 {0.1%}	0.580 {8%}	0.338 {-1.19%}	0.453 {10.3%}	0.601 {0.1%}	0.600 {10%}

[a]Relative percentage errors of prediction

5. Discussions

5.1. Single-cracked beam

As it is observed in the Figures and Table 3 of single-cracked beam, for cracks of depths 0.1 and 0.2, $R_2^{(n,1)}$ function has the maximum closeness to $W^{(n,1)}$ values for almost all crack locations. At majority of locations, by increasing the depth of the crack, the closeness between $R_2^{(n,1)}$ and $W^{(n,1)}$ decreases, as far as the $R_1^{(n,1)}$ function leads to better results than the $R_2^{(n,1)}$, for the case of the first mode and $\gamma = 0.5$. In the second mode, for the depths less than 0.2, $R_2^{(n,1)}$ gives us more exact results. However, for the depths equal to 0.3 and higher, by

increasing the crack location β equal to 0.7 and 0.8, the closeness between $R_2^{(n,1)}$ and $W^{(n,1)}$ decreases. Thus, at the neighborhood of the tip of the beam, $R_1^{(n,1)}$ function gives us more accurate results. On the other hand, in the second mode, for $\beta = 0.2$ and less, $R_2^{(n,1)}$ function gives us better results than $R_1^{(n,1)}$. We can see the experimental results of the above discussion in Table 3. We can conclude from the above discussion and Table results that the modified function $R_2^{(n,1)}$ leads to better results than $R_1^{(n,1)}$ for the following cases:

1) Small depth cracks (about $\gamma \le 0.2$). As some examples, see Table 3, the cases no. 1 to 4.

2) Cracks near to the root of a beam, in the range of $\beta \le 0.2$, including both low and high depth cracks. As an example, see Table 3, the case no. 10.

According to the above discussion, we find that by increasing crack depth, the accuracy of $R_2^{(n,1)}$ function decreases. We can find the reason for this in Eq. (19). According to this equation, by increasing the crack depth, the effect of corrective coefficient increases as well. For example, for $\gamma = 0.1$ the correction coefficient is 0.9, while for $\gamma = 0.5$ this coefficient is 0.5. Therefore, we predict that for high severity cracks, this correction factor may follow the variations in $W^{(n,1)}$ more sluggishly.

5.2. Double-cracked beam

For a double-cracked beam, the discussion for the degree of closeness of $W^{(n,2)}$ and $R_2^{(n,2)}$ would be more complicated due to the mutual effects that the interaction of cracks might have in the modification relations. In this section we conclude that $R_1^{(n,2)}$ and $R_2^{(n,2)}$ functions perform approximately on an equal level. In roughly half of the cases, $R_1^{(n,2)}$ performs better than $R_2^{(n,2)}$, and in the other half, the result is reversed. We remind that the $R_3^{(n,2)}$ function has both modifications. It excels in only a few cases, demonstrating no remarkable advantage over the other two functions (Table 2).

On the other hand, according to the crack detection problem detailed in Table 4, comparing the relative error percentages, and considering the computational complexities, the usage of those modified functions is not recommended for double-crack situations.

6. Conclusions

In this paper, we presented energy analysis of multiple-cracked beams. In our analysis, we used three different functions to model the energy consumed by crack initiation and growth. Furthermore, we used these functions into several single and multiple crack detection problems to elucidate our analysis.

Regarding the discussions in Section 5 and a summary of numerical and simulated results, reflected in the Figures and Tables presented, we conclude that the modifications of energy reduction functions proposed in the literature, do not necessarily lead to more accurate results. Even more striking, we emphasize that the prevalent (classical) energy reduction function yields more satisfactory results in a number of case studies, that this number is by no means ignorable.

In general, the results obtained from the proposed modification functions are reliable only in those cases when cracks have low depth and/or are located near the beam root. Increasing the crack depth or approaching toward the beam tip causes a reduction in the accuracy of the

predictions, as we use modified energy reduction functions, as compared to the prevalent (classical) function.

As the number of cracks increases in a beam, obtaining more acceptable results becomes more stringent by using the modification functions. It is reemphasized that in the case studies that all or most of cracks are low-depth and/or close to the beam root, the modifications in the prevalent (classical) function are effective with more accurate results. However, as this is not a rule, for multiple-crack beams (three cracks and above) these modifications in classical energy reduction function are not recommended.

References

[1] **Grabowska J., Palacz M., Krawczuk M.** Damage identification by wavelet analysis. Mechanical Systems and Signal Processing, Vol. 22, Issue 7, 2008, p. 1623–1635.

[2] **Li B., Chen X. F., Ma J. X., He Z. J.** Detection of crack location and size in structures using wavelet finite element methods. Journal of Sound and Vibration, Vol. 285, Issues 4-5, 2005, p. 767–782.

[3] **Hu J., Liang R. Y.** An integrated approach to detection of cracks using vibration characteristics. Journal of the Franklin Institute, Vol. 330, Issue 5, 1993, p. 841–853.

[4] **Sekhar A. S.** Multiple cracks effects and identification. Mechanical Systems and Signal Processing, Vol. 22, Issue 4, 2008, p. 845–878.

[5] **Chondros T. G., Dimarogonas A. D., Yao J.** A continuous cracked beam vibration theory. Journal of Sound and Vibration, Vol. 215, Issue 1, 1998, p. 17–34.

[6] **Gounaris G., Dimarogonas A.** A finite element of a cracked prismatic beam for structural analysis. Computers & Structures, Vol. 28, Issue 3, 1988, p. 309–313.

[7] **Khiem N. T., Lien T. V.** A simplified method for natural frequency analysis of a multiple cracked beam. Journal of Sound and Vibration, Vol. 245, Issue 4, 2001, p. 737–751.

[8] **Orhan S.** Analysis of free and forced vibration of a cracked cantilever beam. NDT and E International, Vol. 40, Issue 6, 2007, p. 443–450.

[9] **Christides S., Barr A. D. S.** One-dimensional theory of cracked Bernoulli-Euler beams. International Journal of Mechanical Sciences, Vol. 26, Issue 11-12, 1984, p. 639–648.

[10] **Ostachowicz W. M., Krawczuk M.** Analysis of the effect of cracks on the natural frequencies of a cantilever beam. Journal of Sound and Vibration, Vol. 150, Issue 2, 1991, p. 191–201.

[11] **Wang D., Zhu H., Chen C., Xia Y.** An impedance analysis for crack detection in the Timoshenko beam based on the anti-resonance technique. Acta Mechanica Solida Sinica, Vol. 20, Issue 3, 2007, p. 228–235.

[12] **Khaji N., Shafiei M., Jalalpour M.** Closed-form solutions for crack detection problem of Timoshenko beams with various boundary conditions. International Journal of Mechanical Sciences, Vol. 51, Issues 9-10, 2009, p. 667–681.

[13] **Viola E., Federici L., Nobile L.** Detection of crack location using cracked beam element method for structural analysis. Theoretical and Applied Fracture Mechanics, Vol. 36, Issue 1, 2001, p. 23–35.

[14] **Qian G. L., Gu S. N., Jiang J. S.** The dynamic behaviour and crack detection of a beam with a crack. Journal of Sound and Vibration, Vol. 138, Issue 2, 1990, p. 233–243.

[15] **Bovsunovsky A. P., Matveev V. V.** Analytical approach to the determination of dynamic characteristics of a beam with a closing crack. Journal of Sound and Vibration, Vol. 235, Issue 3, 2000, p. 415–434.

[16] **Chondros T. G., Dimarogonas A. D., Yao J.** Vibration of a beam with a breathing crack. Journal of Sound and Vibration, Vol. 239, Issue 1, 2001, p. 57–67.

[17] **Dilena M., Morassi A.** Identification of crack location in vibrating beams from changes in node positions. Journal of Sound and Vibration, Vol. 255, Issue 5, 2002, p. 915–930.

[18] **Chaudhari T. D., Maiti S. K.** Modeling of transverse vibration of beam of linearly variable depth with edge crack. Engineering Fracture Mechanics, Vol. 63, Issue 4, 1999, p. 425–445.

[19] **Rosales M. B., Filipich C. P., Buezas F. S.** Crack detection in beam-like structures. Engineering Structures, Vol. 31, Issue 10, 2009, p. 2257–2264.

[20] Narkis Y. Identification of crack location in vibrating simply supported beam. Journal of Sound and Vibration, Vol. 172, Issue 4, 1994, p. 549–558.

[21] Patil D. P., Maiti S. K. Detection of multiple cracks using frequency measurement. Engineering Fracture Mechanics, Vol. 70, Issue 12, 2003, p. 1553–1572.

[22] Chen X. F., He Z. J., Xiang J. W. Experiments on crack identification in cantilever beams. Society for Experimental Mechanics, Vol. 45, Issue 3, 2005, p. 295–300.

[23] Lee J. H. Identification of multiple cracks in a beam using natural frequencies. Journal of Sound and Vibration, Vol. 320, Issue 3, 2009, p. 482–490.

[24] Lee J. H. Identification of multiple cracks in a beam using vibration amplitudes. Journal of Sound and Vibration, Vol. 326, Issues 1-2, 2009, p. 205–212.

[25] Chasalevris A. C., Papadopoulos C. A. Identification of multiple cracks in beams under bending. Mechanical Systems and Signal Processing, Vol. 20, Issue 7, 2006, p. 1631–1673.

[26] Khiem N. T., Lien T. V. Multi-crack detection for beam by the natural frequencies. Journal of Sound and Vibration, Vol. 273, Issue 2, 2004, p. 175–184.

[27] Patil D. P., Maiti S. K. Experimental verification of a method of detection of multiple cracks in beams based on frequency measurements. Journal of Sound and Vibration, Vol. 281, Issues 1-2, 2005, p. 439–451.

[28] Yang X. F., Swamidas A. S. J., Seshadri R. Crack identification in vibrating beams using the energy. Journal of Sound and Vibration, Vol. 244, Issue 2, 2001, p. 339–357.

[29] Behzad M., Meghdari A., Ebrahimi A. A new approach for vibration analysis of a cracked beam. International Journal of Engineering, Vol. 18, Issue 4, 2005, p. 319–330.

[30] Mazanoglu K., Yesilyurt I., Sabuncu M. Vibration analysis of multiple-cracked non-uniform beams. Journal of Sound and Vibration, Vol. 320, Issues 4-5, 2009, p. 977–989.

[31] Mazanoglu K., Sabuncu M. Vibration analysis of non-uniform beams having multiple edge cracks along the beam's height. International Journal of Mechanical Sciences, Vol. 52, Issue 3, 2010, p. 515–522.